

Formation and decay of intramolecular exciplexes and bond homolysis of ((*N,N*-dimethylamino)methyl)arenes

S. Schneider ^{a,*}, H. Rehaber ^a, W. Schüßlbauer ^a, F.D. Lewis ^{* b}, B.A. Yoon ^b

^a Institut für Physikalische und Theoretische Chemie, Friedrich-Alexander-Universität, D 91058 Erlangen, Germany

^b Department of Chemistry, Northwestern University, Evanston, IL 60208-3113, USA

Received 7 February 1996; accepted 28 March 1996

Abstract

This contribution reports on the photophysical and photochemical behavior of several ((*N,N*-dimethylamino)methyl)arenes. Monomer (arene) fluorescence is strongly quenched by efficient intramolecular charge transfer from the amino to the arene group. The properties of the resulting exciplexes vary considerably with the arene moiety, the position of attachment of the amino group and with solvent polarity. All of the compounds investigated show photochemical decomposition by σ (CN) bond cleavage. It is suggested that the CT state is precursor to the dissociative $^3\sigma^*(\text{CN})$ state.

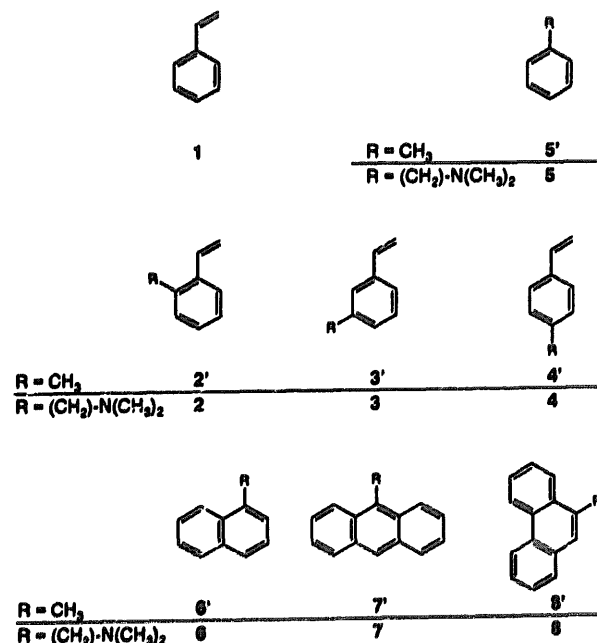
Keywords: Photoinduced electron transfer; Exciplex fluorescence; Intersystem crossing; Radical formation

1. Introduction

The formation of intramolecular arene amine exciplexes and their photophysical and photochemical behaviour is a topic of longstanding interest [1–7]. Some of the initial experiments demonstrated that monomer quenching does not always parallel the formation of fluorescing exciplexes and that the steric and other requirements are different for these processes. Exciplex formation and decay was found to be dependent upon several factors, namely: (i) the redox properties of the amine donor and the arene acceptor moiety, (ii) the chain length of the (flexible) aliphatic bridge between them, (iii) the point of attachment of the bridge onto the arene and (iv) the solvent polarity.

Most previous investigations have focused on systems with two or more methylene groups in the bridge since the corresponding aminomethyl arenes ($n=1$) were reported to exhibit no or only a very weak exciplex fluorescence [1,3,5,7]. As a consequence, only little is known about the excited state kinetics of the various aminomethyl arenes, although their behaviour should be interesting due to the expected strong through-bond and through-space interaction, caused by the short distance between electron donor and acceptor. It has been speculated that exciplex fluorescence in those systems is quenched by intramolecular bond formation [2]. Based on their photolysis studies on dibenzylamines,

Ratcliff and Kochi [8] postulated photoinduced bond cleavage and formation of benzyl and dimethylamino radicals from **5** (see Chart 1 below for structures and abbreviations of compounds under investigation). Furthermore, it was shown that in linked styrene and stilbene amine systems with $n \geq 2$ photoinduced hydrogen transfer occurred from the α -carbon,



* Corresponding authors.

the efficiency of this reaction being sensitively dependent upon chain length and solvent polarity [5].

In two recent publications we could show that the aminomethyl styrenes **2** and **4** [7] and the aminomethyl phenanthrene **8** [6] show weak exciplex fluorescence and undergo $\text{ArCH}_2\text{-NMe}_2$ cleavage reaction. In this contribution we give a more detailed report of the results of our collaborative investigations of several additional aminomethyl arene systems (see Chart 1) and with special emphasis on the mechanism of C–N bond cleavage.

2. Experimental details

2.1. Materials

Styrene (**1**), *ortho*-methylstyrene (**2'**), *meta*-methylstyrene (**3'**), *para*-methylstyrene (**4'**), *N,N*-dimethylbenzylamine (**5**), toluene (**5'**), 1-methylnaphthalene (**6'**), 9-methylantracene (**7'**) and bibenzyl were purchased from Aldrich Chemical Co. The syntheses of 9-((*N,N*-dimethylamino)methyl)phenanthrene (**8**) and 9-methylphenanthrene (**8'**) have previously been described in reference [6], those of *ortho*-(**2**) *meta*-(**3**) and *para*-(**4**) ((*N,N*-dimethylamino)methyl)styrene in references [9]a and [9]b.

1-((*N,N*-dimethylamino)methyl)naphthalene (**6**). Reductions of 1-naphthonitrile (0.92 g, Aldrich) with excess LiAlH_4 in diethylether provided 1-(aminomethyl)naphthalene (0.82 g, 89% yield). Reductive methylation of this amine using the method of Borch and Hassid [10] afforded 1-((*N,N*-dimethylamino)methyl)naphthalene as a colorless oil in 93% yield: $^1\text{H-NMR}$ δ 8.25 (d, 1H, $J=8.4$ Hz), 7.85 (d, 1H, $J=8.4$ Hz), 7.76 (m, 1H), 7.39–7.53 (m, 6H), 3.81 (s, 2H), 2.30 (s, 6H). HRMS 185.1205 (clcd) and 185.1187 (obsd).

9-((*N,N*-dimethylamino)methyl)anthracene (**7**). Reductive methylation of 9-((*N*-methylamino)methyl)anthracene (Aldrich) by the method of Borch and Hassid afforded 9-((*N,N*-dimethylamino)methyl)anthracene as a pale yellow solid: m.p. 66–67 °C; $^1\text{H-NMR}$ δ 8.47 (s, 1H), 8.46 (d, 2H, $J=6.6$ Hz), 8.00 (d, 2H, $J=6.6$ Hz), 7.50 (m, 4H), 4.38 (s, 2H), 2.38 (s, 6H). MS (m/e): 185.1 (M^+).

2.2. Experimental methods

NMR spectra were recorded in CDCl_3 solutions using a Gemini 300 Varian spectrometer with TMS as an internal standard. Mass spectra were determined on a Hewlett-Packard 5985 GC/VG70-250SE MS apparatus with an ionizing voltage of 70 V. Melting points were measured on a Fisher-Johns apparatus and are uncorrected. Ultraviolet absorption spectra were recorded on a Hewlett-Packard 8452A diode-array and Perkin Elmer (Model Lambda 2) absorption spectrophotometer. Steady-state fluorescence spectra were obtained on a Spex Fluoromax or Perkin Elmer (Model LS50) spectrometer. Lifetime data were collected by means

of a home-built instrument using the frequency-doubled output of a synchronously pumped mode-locked dye laser for excitation. Conventional single-photon-timing technique was employed for recording the fluorescence decay curves. Instrumental response was 100 ps fwhm. The decay parameters were determined for single decay curves by a least-squares fit routine and their quality judged by the reduced χ^2 – values as well as by the randomness of the weighted residuals. All solvents were distilled prior to use. Solutions were about 10^{-4} M and purged with argon for 10 min.

Preparative-scale irradiations were carried out under nitrogen in quartz or Pyrex test tubes using a Rayonet reactor fitted with lamps with maxima at 254 nm (for irradiation of **2–5**), 300 nm (for irradiation of **6**), or 350 nm (for irradiation of **7**). Quantum yield measurements were carried out in the Rayonet reactor using *trans*-stilbene as the actinometer [11]. Irradiated solutions were analyzed for product formation using a Hewlett-Packard 5890 gas chromatograph equipped with a flame ionization detector and a 10×0.53 mm² fused silica column coated with polymethyldisiloxane.

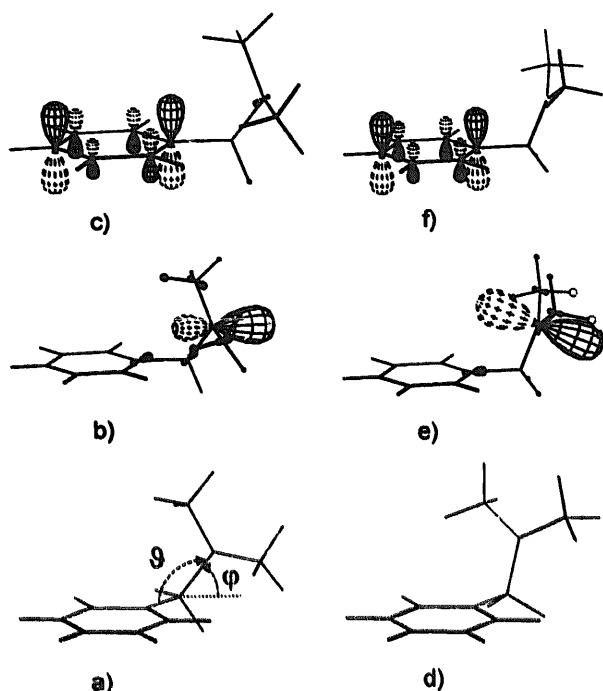
2.3. Product identification

Deoxygenated hexane solutions (0.01 M) were irradiated and monitored by gas chromatography. After ~90% conversion of starting material, the solvent was removed and the residue chromatographed on silica gel preparative thick layer plates. The isolated products were identified by $^1\text{H-NMR}$ and HRMS. The methylarene products **2'–7'** and bibenzyl were identified by comparison with commercial samples. The 1,2-diarylethane products from **4** and **6** were characterized as follows: 1,2-(di-*p*-styryl)ethane: $^1\text{H NMR}$ δ 7.24 (d, 4H, $J=7.8$ Hz), 7.14 (d, 4H, $J=8.1$ Hz), 6.70 (m, 2H), 5.17 (d, 2H), 5.20 (d, 2H), 2.90 (s, 4H). HRMS 234.1408 (clcd) and 234.1402 (obsd). 1,2-(di-1-naphthyl)ethane: $^1\text{H-NMR}$ δ 8.14 (d, 2H, $J=7.9$ Hz), 7.91 (d, 2H, $J=8.0$ Hz), 7.76 (d, 2H, $J=8.2$ Hz), 7.38–7.56 (m, 8H), 3.53 (s, 4H). HRMS 282.1409 (clcd) and 282.1419 (obsd). Also isolated from the irradiation of **5** in diethylether was 2-ethoxy-1-phenylpropane: $^1\text{H-NMR}$ δ 7.15–7.35 (m, 5H), 3.39–3.65 (m, 3H), 2.95 (m, 1H), 1.13 (d, 3H, $J=7.1$ Hz). $^{13}\text{C-NMR}$ 138, 129, 127, 126, 76, 63, 42, 19, 15. HRMS 164.1196 (clcd) and 164.1190 (obsd).

2.4. Quantum-chemical model calculations

Semi-empirical quantum-chemical model calculations were performed by means of the program package VAMP 5.5 [13]a using the PM3 Hamiltonian [13]b. First, energy optimized geometries were calculated for the ground state of a molecule (ground state conformation, GSC).

With these geometries, CI calculations were performed including all singly and doubly excited configurations, which can be constructed from the 5 highest occupied and 5 lowest unoccupied SCF orbitals. The resulting wavefunctions describe the locally excited (LE) states.



Scheme 1. Calculated minimum energy ground state conformation (GSC) of **5** (a) and corresponding HOMO (b) and LUMO (c). Compact CT state conformation (CTC) (d) and corresponding HOMO (e) and LUMO (f).

In order to calculate the properties of the exciplexes, a 'compact' geometry is generated. The torsional angle of the bond between methylene group and arene, φ , is fixed at 90° thus leading to the closest distance possible between the nitrogen atom and the C(ipso) of the phenyl ring (compare, e.g., the harpooning mechanism [4]c). At the same time, the pyramidalisation of the $N(CH_3)_2$ group is released. The latter geometry change is assumed in accordance with the observation that a $^+NR_3$ group is planar. With these two parameters fixed, the other bond lengths and angles were optimized to yield a minimum energy conformation (charge transfer conformation, CTC).

This procedure and its results are demonstrated in Scheme 1 for the case of the benzyl derivative **5**. It will be discussed in more detail below.

3. Results and discussion

3.1. Absorption spectra

For the sake of convenience and easier comparison, the UV/VIS absorption spectra of compounds **2–7** are displayed in Fig. 1 and Fig. 2. Also included are the absorption spectra of the corresponding methyl derivatives. In case of compounds **6** and **7**, the absorption spectra of the linked arene amine systems closely match those of the corresponding methyl substituted derivatives. The easily detected, large difference between the spectra of **5** and **5'** (absorption around 230 nm) is due to the absorption originating from the amino

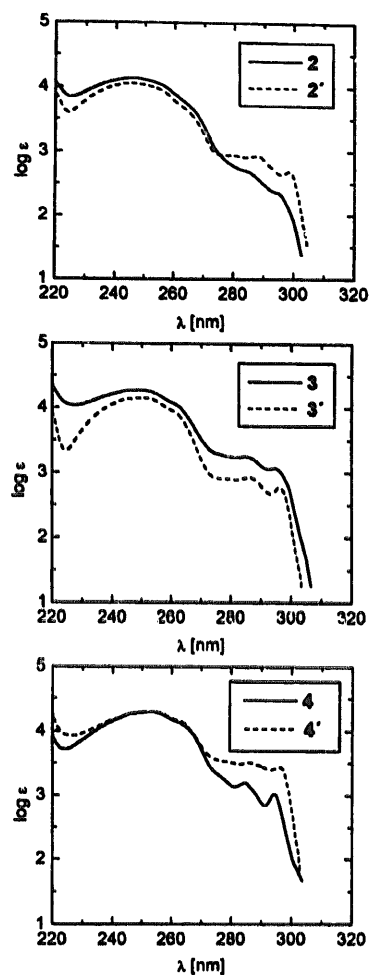


Fig. 1. UV/VIS absorption spectra of the (aminomethyl)styrenes **2–4** (*ortho*, *meta*, *para*) and the corresponding methyl styrenes **2'–4'** in cyclohexane.

group. The aminomethyl substituted compounds **5–7** all exhibit a bathochromic shift of the 0–0 transition into the S_1 state of about 500 cm^{-1} versus the corresponding unsubstituted arene.

In case of the styrene derivatives **2–4**, similar conclusions can be drawn except that in the *ortho* derivative **2**, the weak vibrational structure observed in the longwavelength absorption band (275–300 nm) of **2'** is nearly completely gone. This fact could be simply (i) the consequence of a deviation from a planar geometry due to the steric interaction between the vinyl groups and the amino group and/or (ii) the consequence of a structural heterogeneity. The model calculations predict the existence of two low energy conformers, which can be transformed into each other by a 30° rotation around the single bond between the ipso-C-atom of the ring and the methylene group. For these two conformers, the model calculations predict a difference in excitation energy of about 100 cm^{-1} ($= 1\text{ nm}$) (It should be noted here that Seemann et al. [12] found in jet experiments on anethole (*p*-methoxy) β -methyl styrene) a difference in the lowest singlet excitation energy of 69 cm^{-1} for the two possible conformers). A superposition of the spectra of the two con-

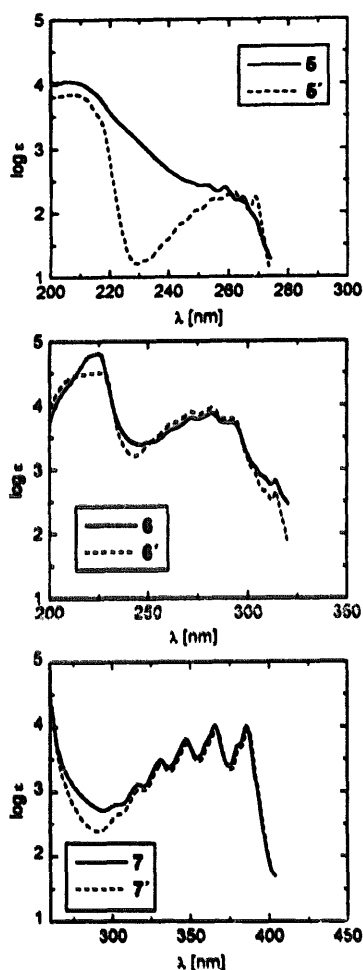


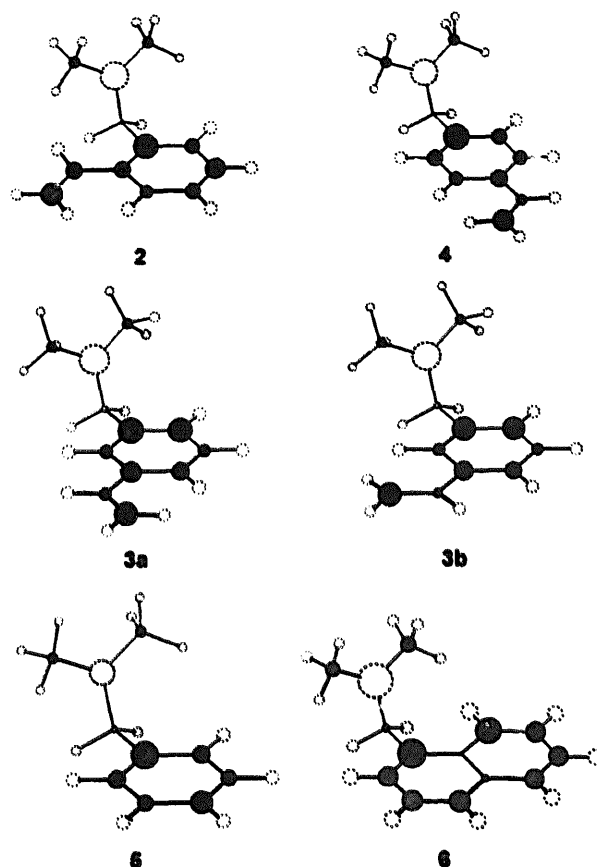
Fig. 2. UV/VIS absorption spectra of the (aminomethyl)arenes 5–7 (benzene, naphthalene, anthracene) and the corresponding methyl arenes 5'–7' (solvent cyclohexane).

formers could therefore lead to a reduction in vibrational structure. On the other hand, the model calculations predict also the existence of two conformers in case of the *meta* derivative 3 (rotation around C(phenyl)–C(vinyl) bond, see Scheme 2) with a similar difference in excitation energy. Since the vibrational structure is conserved to a larger extent in 3 and 4, we believe that the nonplanar arrangement of the vinyl group is the major source for the disappearance of the vibrational structure in the absorption spectrum of 2.

Another important conclusion to be drawn from the absorption spectra is that, as has been pointed out before [1–7], no indication of a charge transfer band can be found in any of the linked arene amine systems under investigation. Photon absorption, therefore, should lead exclusively to the locally excited state.

3.2. Stationary fluorescence

The stationary emission spectra of compounds 2, 3 and 4 recorded in solvents of different polarity are displayed in Fig. 3, those of 6 (THF, acetonitrile) and 7 (acetonitrile) in



Scheme 2. Calculated charge density distributions in the CT state (compact geometry CTC, see Scheme 1) of 2, 3 (two conformations a and b), 4, 5 and 6.

Fig. 4. Some of the important characteristics are summarized in Tables 1 and 2.

In case of the styrene derivatives 2–4, the fluorescence behaviour is dependent upon the position of attachment. In cyclohexane, monomer emission from 3 is nearly completely quenched, it is very weak from 2 and weak from 4. The exciplex emission intensity follows the opposite trend, it is strongest in 3 and not detectable in 4. In more polar solvents, a red-shifted exciplex emission can be observed for all three derivatives. The intensity ratio between monomer and exciplex emission is, however, dependent both on solute and solvent. The determination of monomer fluorescence quantum yields is hampered by two factors: (i) the emission yield is so low that Raman scattered light from the solvent is of comparable intensity and (ii) during the measuring process enough material is decomposed such that photoproducts with higher fluorescence yield cover up the emission of the starting material (see Fig. 5). The spectral distribution of the fluorescence, which grows on irradiation, is identical to that of the corresponding methyl derivatives.

Davidson and Trethewey [3](b) also observed a substitution position dependence of exciplex fluorescence intensity in case of the naphthalene derivatives (α versus β -substitution) but no lifetime data were reported. It has been stressed before [3](b) that different requirements may exist for mon-

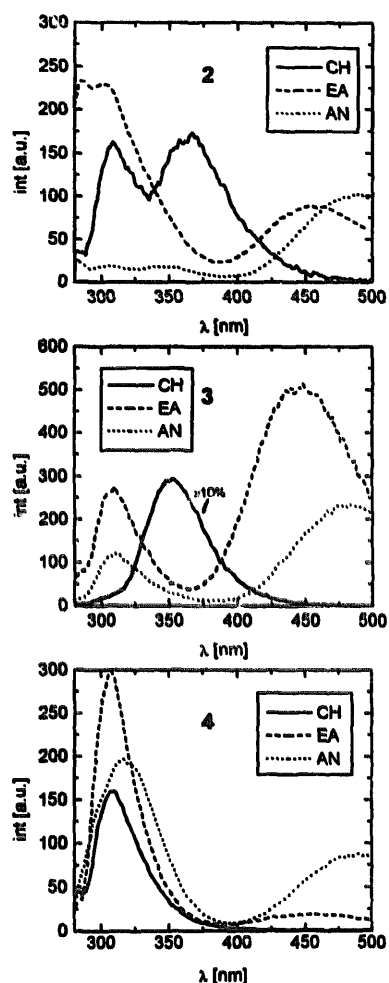


Fig. 3. Emission spectra of styrene derivatives 2–4 in solvents of different polarity (CH: cyclohexane, EA: ethylacetate, AN: acetonitrile); $\lambda_{ex} = 260$ nm.

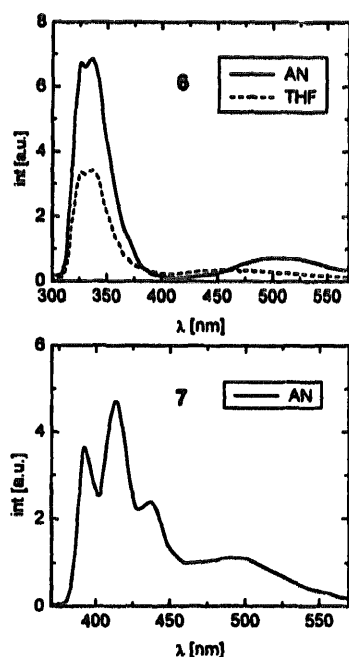


Fig. 4. Emission spectra of the (aminomethyl)arenes 6 ($\lambda_{ex} = 285$ nm) and 7 ($\lambda_{ex} = 350$ nm) (AN = acetonitrile, THF = tetrahydrofuran).

Table 1

Exciplex decay times τ^{ex} (in ns) and exciplex fluorescence maxima λ_m^{ex} (in nm) of the (aminomethyl)styrenes 2, 3 and 4; excitation wavelength in the time-resolved experiment was 265 nm

	2		3		4	
	τ^{ex}	λ_m^{ex}	τ^{ex}	λ_m^{ex}	τ^{ex}	λ_m^{ex}
Cyclohexane	0.39	371	1.64.2	355	–	a
Diethylether	0.84	415	2.44.6	420	b	~420
Ethylacetate	1.03	460	4.38	448	0.36	440
THF	1.00	455	4.25	445	0.36	450
CH ₂ Cl ₂	1.10	443	4.13	438	0.27	430
Acetonitrile	1.47	485	4.19	480	0.79	490

^a Emission not observed.

^b Emission too weak for lifetime measurements.

Table 2

Quantum yields of monomer ($\Phi_f(M)$) and exciplex emission ($\Phi_f(ex)$), exciplex decay times τ^{ex} (in ns) and exciplex fluorescence maxima λ_m^{ex} (in nm) of the (aminomethyl)arenes 6–8 (excitation wavelength in the time-resolved experiment was 285 nm)

Compound	Solvent	$\Phi_f(M)$	λ_m^{ex}/τ^{ex}	$\Phi_f(ex)$
6	hexane	0.003	a	a
	THF	0.014	418	0.003
	acetonitrile	0.004	504	0.001
7	benzene	0.005	a	a
	THF	0.0036	~485	~0.0004
	acetonitrile	0.016	~498	~0.0005
8 ^c	hexane	–	a	–
	diethylether	–	444/b	–
	ethylacetate	–	470/b	–
	THF	–	450/3.4 ns	–
	acetonitrile	–	500/1.1 ns	–

^a Exciplex emission not observed.

^b Emission too weak for lifetime measurements.

^c Data from ref. [6] for comparison.

omer quenching by exciplex formation to be efficient and for exciplexes to exhibit detectable fluorescence (radiative charge recombination). The series of compounds presented in this investigation provides further evidence for this fact. In accordance with prior reports [3], we found in all solvents used a weak monomer emission ($\Phi_f(M) \leq 0.015$) for 6 and 7. Extremely weak exciplex emission could be detected in medium and strongly polar solvents. For the benzyl derivative 5, in accordance with reference 2, neither monomer nor exciplex emission could be detected of freshly prepared, non-irradiated solutions independent of solvent and temperature.

Triethylamine quenches the methylarene fluorescence in nonpolar solvents by intermolecular exciplex formation, although sometimes with rate constants well below diffusion controlled. Intermolecular exciplex fluorescence in unpolar solvents is, however, not observed for the larger arenes like anthracene or phenanthrene. In more polar solvents, the lack of exciplex fluorescence is explained as a consequence of rapid cage escape and formation of free radical ions. In the linked systems, complete separation of the radical ions is not

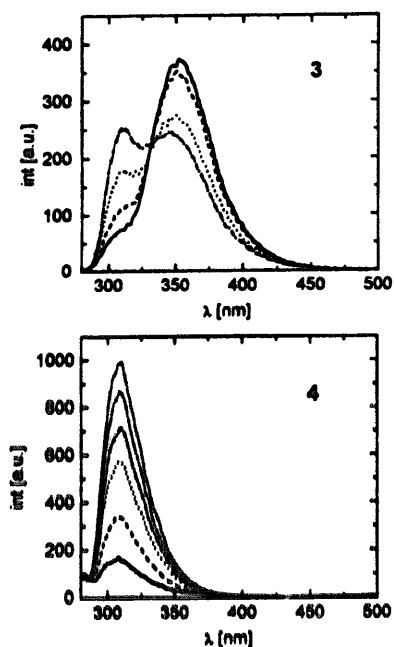


Fig. 5. Effect of irradiation on fluorescence spectrum of 3 and 4 in cyclohexane (with increasing time of irradiation, the emission intensity around 315 nm increases); λ_{ex} was 260 nm.

possible, except that in strongly polar solvents the exciplex can adopt a less compact conformation with less overlap of the orbitals involved in the charge transfer process. This orbital overlap is, in most cases, a necessary requirement for high exciplex fluorescence yields. The strongest exciplex emission from linked systems is therefore expected and actually observed in solvents of moderately high polarity (see Table 2), in which the exciplex is sufficiently strongly stabilized versus the locally excited state. In nonpolar solvents, intramolecular exciplex formation can be prohibited in cases where intermolecular exciplex formation is energetically allowed. The reason for this difference in behaviour must be sought in the geometric restriction introduced by the bridge, which does not allow an optimal approach of the small donor orbital (nitrogen lone pair) onto the accepting, delocalized π^* -system of the arene. But this fact should also explain the variations of exciplex fluorescence with arene size and position of attachment. Discussions along this line have been presented for systems with longer aliphatic chain bridges [3–5] but not applied to the shortest homologues, where the discussed effects could be of even larger importance.

3.3. Exciplex energies and dipole moments

The change in free enthalpy upon exciplex formation, ΔG_{et} , is usually estimated by applying Weller's equation [14]

$$\Delta G_{et} = E(D^+/D) - E(A/A^-) - E_{0,0} + \Delta E_{coul} \quad (1)$$

with: $E(D^+/D)$ = oxidation potential of donor, $E(A/A^-)$ = reduction potential of acceptor, $E_{0,0}$ = excitation energy of acceptor (donor), ΔE_{coul} , which describes the con-

tribution of solvation of the ion pair, is approximated by $\Delta E_{coul}(n\text{-hexane}) = 0.38$ eV and $\Delta E_{coul}(\text{acetonitrile}) = -0.06$ eV. It was mentioned above that methyl substitution shifts the absorption spectra, but it also changes the reduction potentials of the arenes. Both factors lead to a free energy change ΔG_{et} , which is less exergonic (more endergonic) than that of the unsubstituted compounds. The calculated values for ΔG_{et} listed in Table 3, for *n*-hexane and acetonitrile as solvents, can explain why the monomer quenching of the larger arenes in cyclohexane is much less efficient than that of naphthalene and especially that of the styrenes. Furthermore, it is evident that monomer quenching should occur efficiently in solvents of medium to high polarity, in accordance with experimental observation. The reduction potential of benzene or toluene is too negative to be determined experimentally under conventional conditions (e.g. electrodes, solvents). Although there are no definite values of reduction potential, one can nevertheless predict that electron transfer is very highly exergonic and concomitantly a very efficient monomer quenching occurs in non-polar solvents.

Intramolecular exciplex formation in nonpolar solvents should be endergonic in arene systems larger than naphthalene, for which reason monomer emission should appear only weakly quenched. It has been shown that in case of the intermolecular exciplex between TEA and styrene (1) exciplex formation occurs as a fairly reversible reaction in cyclohexane [16]. Methyl substitution and linkage of the amino group to the styrene lead to a smaller exergonicity of the electron transfer (see discussion above). In this solvent, electron back-transfer could, therefore, be an important process also in the decay of the intramolecular exciplexes 2, 3 and 4. Because of the smaller exergonicity, which can be expected for the larger arene amine systems (see discussion above), an even higher reversibility of the charge transfer should be expected in these compounds than in the styrene amine sys-

Table 3

Calculated free energy ΔG_{et} (in eV) for intermolecular arene/TEA exciplex formation; $E(D^+/D)$ (TEA) = 1.15 eV^a; $E_{0,0}$ and $E(A/A^-)$ (vs. SCE) in eV

Compound	$E_{0,0}$	$E(A/A^-)$	$\Delta G_{et}(n\text{-hexane})$	$\Delta G_{et}(\text{acetonitrile})$
1	4.26 ^d	-2.58 ^b	-0.15	-0.59
4'	4.20	-2.66 ^b	-0.01	-0.45
Naphthalene	3.99	-2.49 ^c	0.03	-0.41
6'	3.94	-2.58 ^c	0.17	-0.27
Anthracene	3.27	-1.95 ^c	0.21	-0.23
7'	3.21	-1.97 ^c	0.30	-0.14

^a vs. SCE in acetonitrile ref. [19].

^b Reduction potential measured as -2.60 V (1) and -2.68 V (4') vs. Ag/AgCl in acetonitrile, ref. [18].

^c in DMF, ref. [19]; the values in DMF are used because there are only little differences in dielectric constants (at 295 K) of acetonitrile ($\epsilon = 35.94$) and DMF ($\epsilon = 36.71$), ref. [20].

^d In the literature, often not the energy of the long wavelength absorption but the energy of the 0-0 transition of the α -band (4.47 eV) is cited.

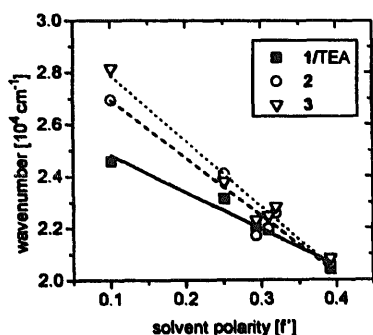


Fig. 6. Variation of exciplex fluorescence maximum with solvent polarity (Lippert–Mataga plot). Solvent polarity parameter f' is defined by Eq. 3.

$$\begin{aligned}\bar{\nu}(1/\text{TEA}) &= 6200-14200 \text{ cm}^{-1} * f' \\ \bar{\nu}(2) &= 29200-22310 \text{ cm}^{-1} * f' \\ \bar{\nu}(3) &= 30450-25380 \text{ cm}^{-1} * f'\end{aligned}$$

tems. However, entropic effects could promote the primary charge separation.

In polar solvents, the destabilizing interactions induced by the bridge should not be large enough to make the electron transfer process significantly less exergonic than in the intermolecular case (strong monomer fluorescence quenching).

The solvent dependent stabilisation of the exciplex is best demonstrated in a Lippert–Mataga plot (Fig. 6), which provides a relationship between the dipole moment μ_e of the emitting state and the wavenumber of the charge transfer emission maximum [15]

$$\bar{\nu}_{\text{CT}} = \bar{\nu}(0) - \frac{\mu_e^2}{2\pi h \epsilon_0 a_0^3} \quad (2)$$

$\bar{\nu}_{\text{CT}}$ and $\bar{\nu}(0)$ are emission wavenumbers in solution and in the gas phase, a_0 is the radius of the cavity occupied by the molecule, h is Planck's constant, c is the velocity of light and f' the Lippert factor of polarity, which is given in Eq. 3 (ϵ and n are dielectric constant and refractive index of the solvent):

$$f' = \frac{\epsilon - 1}{2\epsilon + 1} - \frac{n^2 - 1}{4n^2 + 2} \quad (3)$$

Despite the fact that there are only a limited number of data points available, it can be concluded that the slope of the regression line is much smaller in the case of the intermolecular exciplex 1/TEA than in case of the intramolecular styrene exciplexes of 2 and 3. If one assumes that the radius of the solvent cage a_0 is the same in all cases, then the dipole moment of the CT state of the intramolecular compounds must be significantly larger than that of the intermolecular exciplex.

Assuming $a_0 = 5 \text{ \AA}$, one gets using the slopes from Fig. 6: $\mu(3) = 18.0 \text{ D}$ (average of the two conformational isomers), $\mu(2) = 16.4 \text{ D}$ and $\mu(1/\text{TEA}) = 13.3 \text{ D}$. This is in accordance with the results of the quantum-chemical model calculation, which yield: $\mu(3) = 14.4 \text{ D}$ and 15.4 D , respectively and $\mu(2) = 12.2 \text{ D}$ (see below).

As mentioned in Section 2.4, we have to anticipate in our calculations the geometrical changes induced by photoindu-

ced electron transfer, since in the program package VAMP no provision is made for calculations of excited state geometries. In Scheme 1, the chosen procedure is illustrated for the benzyl derivative 5. Optimization of the ground state geometry yields a torsional angle $\varphi = 66^\circ$ for the C(phenyl)–C(methylene) bond with an inclination of the C(methylene)–N bond to the phenyl ring of $\vartheta = 116^\circ$. For this geometry, HOMO ($\epsilon_H = -9.02 \text{ eV}$) and LUMO ($\epsilon_L = 0.22 \text{ eV}$) are calculated as displayed in Scheme 1(b) and Scheme 1(c). One electron promotion between these orbitals is therefore truly a charge transfer process. The equivalent calculation, but with the rotation angle φ fixed at 90° and the hybridization of the amino nitrogen changed to sp^2 , yields HOMO ($\epsilon_H' = -8.21 \text{ eV}$) and LUMO ($\epsilon_L' = 0.33 \text{ eV}$) with essentially the same expansion coefficients. Because of the modified distance of the amino nitrogen (electron donor) to the arene moiety (electron acceptor), the calculated excited state dipole moments are subject to significant changes, as are the energies of the CT states relative to those of the corresponding ground states.

It was found that in all systems under investigation except 7 the angles φ and ϑ are similar in the optimized ground state geometry, the barrier for torsion around the C(phenyl)–C(methylene) bond being only of the order of 4 kJ/mol . The anthryl derivative 7 is exceptional because of the large steric hindrance introduced by the two additional (symmetrical) rings. There, the angle φ equals 90° in the optimized ground state geometry.

In the compact CT geometries the angle of inclination ϑ is reduced from 116 to 113° independent of the size of the aryl system. Therefore, in this approximation the overlap between nitrogen lone pair (electron donor) and π^* orbital of the aryl system (electron acceptor) is determined by the expansion coefficient of the LUMO orbital at the ipso-carbon atom.

In Scheme 2, the charge distribution calculated for the assumed CT-state geometries are displayed. It is immediately evident that the amount of charge transferred from the amino group to the arene system varies with the size of the arene moiety (in Scheme 2, the diameters of the circles are proportional to the electronic charge on the corresponding atom).

Especially interesting is comparison of the charge distribution in the substitutional isomers 2–4. The positive charge is located mainly on the nitrogen of the amino group ($q_N \sim 0.52-0.57$), but a significant amount is also found on the methylene bridge ($q_B \sim 0.14$) and the methyl groups ($q_M \sim 0.10$). In case of 2 and 3, almost the same amount of negative charge ($q_{\text{ipso}} \sim -0.3$) is located on that C-atom of the phenyl ring, to which the methylene bridge is connected and on the β -C-atom of the vinyl double bond. Significant negative charge ($q \sim -0.3$) is found, in addition, at the phenyl carbon atom in *para* position to the vinyl group and at the vinyl substituted carbon atom ($q \sim -0.2$). Therefore, in case of 2 and 3 one important parameter for exciplex

Table 4

Results of quantum-chemical model calculations using the hypothetical compact CT-state (CTC) geometry (for more details see Section 3.3). The reported quantities are $\Delta(\Delta H_f)$: difference in heat of formation for compound in ground state optimized geometry and CTC-geometry; $E(^1CT)$, $E(^3\sigma^*(CN))$: Excitation energies of corresponding states relative to hypothetical ground state in CTC geometry; $\mu(^1CT)$: dipole moment of CT state in CTC geometry; $T_1(\text{exp})$ refers to experimentally determined triplet energies of unsubstituted arenes

Compound	$\Delta(\Delta H_f)$	$E(^1CT)$	$\mu(^1CT)$	$E(^3\sigma^*(CN))$	$E(^3Ar^*)$	$T_1^b(\text{exp})$
2	0.33	4.80	12.2	3.39	3.01	2.67
3a	0.34	4.89	14.4	3.41	3.02	2.67
3b	0.35	4.94	15.4			
4	0.33	4.83	14.0	3.39	2.99	
5	0.33	4.75	9.41	3.10	3.29	3.66
6	0.33	4.67	12.24	3.47	2.90	2.64
7	0.26	4.06	12.92	2.81	1.89	1.84
8	0.32	4.43	15.51	2.85	2.48	2.69

^a Because the influence of methyl substitution on the energies of the local T_1 of the arenes is small, the T_1 energies of the unsubstituted species are listed.

^b ref. [19].

stabilization is the distance between the positive charge at the amino nitrogen and the negative partial charge on the β -C-atom of the styrene anion. It is obvious that this distance is greater in **3** (note, that the two isomers have different distances) than in **2**. As a consequence, the exciplex of the *ortho* derivative is stabilized better, as manifested in the large separation of monomer and exciplex emission in cyclohexane. This shift is smaller in case of **3** (Fig. 3). In polar solvents, where dipolar interactions with the solvent are strong, Coulombic interaction within the exciplex is not as important as in unpolar solvents. This leads to a similar stabilization and concomitantly similar emission wavelength of these two derivatives.

In the *para* derivative **4**, the negative charge accumulates at the carbon atom to which the bridge is linked ($q \sim -0.43$). This leads to a smaller dipole moment (14.0 D) than expected for the great distance between the amino group and the β -C-atom of the styrene moiety. Because the charge separation is smaller than for the *meta* derivative **3**, one should expect the exciplex of **4** to be of lower energy than that of **3**. The model calculations treating the molecules in the gas phase confirm these considerations. The higher the dipole moment, the higher the exciplex energy (note that this effect leads to a difference in the exciplex energies of the two conformations of **3** of 0.05 eV). But in contrast to **2** and **3**, no exciplex fluorescence can be seen from **4** in cyclohexane.

The conclusion to be drawn from this consideration is that the dipole moment of the CT state or its expected stabilization is not a sufficient criterion to make a prediction whether or not one observes CT emission. It rather seems that it is the actual form of the wavefunctions which makes the difference. (The CI calculations confirm that HOMO and LUMO are the essential orbitals for describing the charge transfer excitation). The expansion coefficients of the LUMO at the ipso-C-atom are 0.47 (**4**), 0.45 (**2**) and 0.22 (**3**). To a first approximation, one would expect the highest rates for radiative charge recombination (CT-fluorescence) in **4** and **2**, and the lowest in **3**. But this is not in accordance with observation. One must, however, keep in mind that a large overlap

between the LUMO located on the phenyl ring and the HOMO located the nitrogen lone pair not only increases the rate for radiative deactivation but also increases the intersystem crossing rate. Therefore, the energetic separation between the states involved is of significance besides the orbital overlap. Radiationless deactivation must therefore dominate in **4**.

In more polar solvents, the change in Coulombic interactions and specific solvation lead to slightly different exciplex geometries. As a consequence of these changes and the variations in the energy gaps between exciplex and triplet or ground state, the ratio of the various rates is dependent upon solvent polarity. In addition, the differences in electronic charge distribution do not lead to different exciplex emission wavelengths of **2**, **3** and **4**, as observed in nonpolar solvents.

In compounds **5–8**, the overlap between electron donating and accepting orbital seems to be similar to that of **4**. A large MO coefficient and concomitantly a high value of negative charge on the ipso-C-atom is found (see Scheme 2). The energetic situation in these compounds must therefore also be favourable for radiationless transitions (see Table 4) and thus accounting for the absence of exciplex fluorescence in nonpolar solvents.

3.4. Time-resolved measurements

Time-resolved measurements of the monomer emission of many of the linked aminomethylene systems suffer from its very low intensity. Small amounts of impurities, which can originate from photoproducts (see later) make the interpretation of the results difficult. In addition, in case of the linked styrene systems Raman scattered light from the solvent is superimposed on the monomer emission since it is difficult to generate excitation pulses at shorter wavelength than 286 nm. Therefore, the following discussion concentrates on exciplex decay times which could be determined for **2** and **3** in cyclohexane and for **2**, **3**, **4** and **8** in the more polar solvents (Tables 1 and 2). The exciplex decay time of **4** in cyclohexane, which was published in a previous paper [7], could not

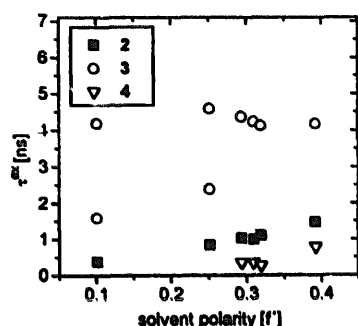


Fig. 7. Variation of exciplex decay time of compounds 2, 3 and 4 with solvent polarity; solvent polarity parameter f' is defined by Eq. 3.

be confirmed because of the reasons discussed above. For compounds 5–7 no lifetime measurements were possible.

It has been pointed out before that methyl substitution of styrene has only small effects on the fluorescence quantum yields and fluorescence decay times of the monomers and the corresponding TEA exciplexes [16], e.g. the decay time of the TEA exciplex in cyclohexane is 17.6 ns for 1/TEA and 13.6 ns for 4³/TEA. In the intramolecular linked systems 2 and 4, one observes much shorter exciplex decay times, which increase with increasing solvent polarity (Fig. 7). In case of the *meta* derivative 3, the reduction of the exciplex decay time is more moderate. Note that the exciplex emission of 3 exhibits a biexponential decay in both the nonpolar solvent cyclohexane and the medium polar solvent diethylether. The difference of the two decay rates becomes smaller when going from cyclohexane to diethylether. In even more polar solvents, the fluorescence decay appears monoexponential. In our opinion, the biexponential decay observed in unpolar solvents is a direct consequence of the existence of two isomers (as discussed above). In nonpolar solvents, the attractive interaction between the partial charges at the vinyl group and the nitrogen contributes significantly to the stabilization of the exciplex. Since the distance between these two locations is different in the two isomers, a significantly different stabilization is achieved which, in turn, results in different decay rates. In polar solvents, the decay times become approximately equal because Coulombic interactions are of less importance. In the *ortho* derivative, the differences are obviously too small to be resolved.

The exciplex decay times of 5, 6 and 7 unfortunately could not be determined. The decay time of the intramolecular exciplex of the phenanthrene derivative 8 decreases from about 3.4 ns in THF to about 1.1 ns in acetonitrile. In the case of intermolecular systems, exciplex decay times are usually shortened in more polar solvents due to the possibility of formation of separated radical ion pairs. A similar effect can be observed in systems where the amine is connected to the arene via a longer, flexible or semiflexible aliphatic chain. In polar solvents, a transition from a compact to an extended exciplex occurs. But neither the formation of separated radical ions nor formation of an extended exciplex is possible in derivative 8. Obviously, one can not easily predict the behaviour of systems with short links. By changing the donor and/

or the acceptor opposite effects are possible at fixed chain length.

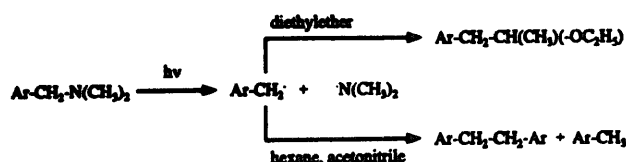
In general, there are many possible decay pathways of the exciplexes of the systems investigated. (i) Due to the close proximity of electron donor and acceptor, not only charge separation but also charge recombination producing ground state molecules should be very fast. (ii) Because the energetic stabilization of the exciplexes relative to the locally excited states is small in unpolar solvents, electron back transfer to the locally excited state could be very important. (iii) Intersystem crossing to the locally excited triplet state can also be an important decay path. In a previous study we reported [5]c that for α - and β -(aminomethyl)styrenes both monomer and exciplex emission were too weak to be studied in either polar or nonpolar solvents. In the case of the β -derivative, the quantum yield for photoisomerization was measured ($\phi_{\text{iso}}^{\text{exc}} = 0.35$) and used to estimate the exciplex intersystem crossing rate ($k_{\text{ISC}}^{\text{exc}} \geq 7 \times 10^9 \text{ s}^{-1}$). In the ((*N,N*-dimethylamino)methyl)pyrene system, Okada et al. observed a very high ISC yield [17], which is solvent sensitive. It is higher in the nonpolar solvent *n*-hexane than in the polar solvent acetonitrile. The high ISC yield is attributed to an approximately perpendicular arrangement of the accepting and donating MOs. Spin-orbit interactions will become enhanced in the perpendicular configuration. The donating orbital (n -orbital of the amino group) and the accepting orbital (π^* -orbital of the arene system) are nearly perpendicular in the assumed compact (folded) conformation. Because of dipolar interaction with the solvent, the arrangement of donor and acceptor is less compact in acetonitrile leading to less ISC via the charge transfer state.

In all systems investigated, these three reaction channels certainly play a role. However, which one is the predominant decay pathway has not been elucidated.

3.5. Photoinduced reactions

Early investigators of the photochemistry of (aminomethyl)arenes considered the possibility that the efficient quenching of the arene fluorescence might result from chemical reactions. Chandross and Thomas [1] suggested that addition of the amino group at the ipso position of 6 formed a thermally unstable spiroazetine intermediate and Bryce-Smith et al. [2] suggested an analogous decay process for 5. Ratcliff and Kochi reported, as unpublished work, the occurrence of benzyl-nitrogen homolysis upon irradiation of 5 with 254 nm light and later reported a detailed investigation of benzyl-nitrogen homolysis of dibenzylamine [8].

We found that irradiation of the (aminomethyl)arenes 2–8 in deoxygenated hexane or acetonitrile solution results in the formation of methyl arenes and 1,2-diarylethanes as the major products. Irradiation in ether solvents also results in the formation of solvent adducts. For example, irradiation of 5 in diethylether results in the formation of 2-ethoxy-1-phenylpropane. These products are presumed to be formed via photolysis of the arylmethylene–nitrogen bond to yield the



Scheme 3. Proposed reaction scheme for photoinduced CN bond cleavage and product formation.

arylmethyl–dimethylaminy radical pair which can disproportionate to yield the methyl arene or undergo cage escape. The resulting arylmethyl radical can abstract hydrogen from the solvent, dimerize to yield the 1,2-diarylethane, or react with solvent-derived radicals (Scheme 3). Quantum yields for the formation of these products are reported in Table 5. Minor products which contain the arylmethyl fragment have been detected by gas chromatography–mass spectroscopy, but not isolated and fully characterized.

As was mentioned already in Section 3.2, photoproduct formation is clearly seen in the fluorescence emission spectra recorded in dependence of time of photolysis (Fig. 5). The emission maximum of the photoproduct is identical to that of the corresponding methyl derivative. Furthermore, the decay time of one component, whose relative amplitude increases with photolysis (e.g. $\tau(4)$ in cyclohexane: 10.5 ns) also matches closely the fluorescence lifetime of the corresponding methyl derivatives ($\tau(4')$ in cyclohexane: 12.5 ns). Under the experimental conditions of these experiments (10^{-4} M solutions), reaction between primarily formed radicals to yield the corresponding 1,2-distyrylethanes can obviously be neglected.

Simple MO considerations suggest that the dissociative excited state, which leads to a homolytic CN bond cleavage, must be the (localized) triplet excited state of the $\sigma(\text{CN})$ bond, $^3\sigma^*(\text{CN})$. The model calculations predict (for all compounds investigated) such an excited state to lie more than 1 eV (8000 cm^{-1}) below the singlet CT-state (cf. Table 4).

The $^3\sigma^*(\text{CN})$ state can not be excited directly by photon absorption, but it could be populated via internal conversion from the triplet charge transfer state, ^3CT , or from the locally excited arene triplet state, $^3\text{Ar}^*$. Alternatively, it could be generated via intersystem crossing from the singlet excited arene state, $^1\text{Ar}^*$, or the singlet charge transfer state ^1CT .

In order to differentiate experimentally between the various possibilities, one can look for correlations between exciplex decay and product formation.

If S_1 were the precursor state for $^3\sigma^*(\text{CN})$, efficient CT state formation should reduce product formation, whereas if the CT state were the precursor, product formation should parallel CT formation. If the arene triplet state were important, then high product yields require a high yield for CT formation and an efficient decay of the CT state into the local triplet (it is assumed that ISC is not an important decay channel of the arene singlet state).

One can speculate that, since fluorescence of the locally excited arene is strongly quenched, the resulting exciplexes play an important role in the cleavage reaction. However, in

many cases exciplex formation is highly reversible in non-polar solvents. Therefore, bond cleavage could in principle occur also via the locally excited singlet state. By increasing the solvent polarity, the exergonicity of exciplex formation increases, its formation is less reversible or may even be irreversible. As a consequence, the probability for dissociation via the S_1 state should be reduced and concomitantly the yield of reaction products lowered, as is observed in all compounds except 7. In the case of 7, where ΔG_{et} is approximately slightly positive, a high yield of products should be obtained if S_1 was the reactive (precursor) state. However, very low yields are obtained for 7 and in hexane the yield is even lower than in acetonitrile. Although we can not exclude the singlet reaction pathway in all cases, it seems unlikely to us. Then the question remains: Is the exciplex state the precursor or is it a locally excited triplet state, which is formed from the charge transfer state? Because the decay times of the exciplexes are very short, quenching experiments with, e.g., primary amines would fail to directly prove this reaction pathway. If the bond cleavage occurred via the CT state, one would expect that bond cleavage and concomitantly the quantum yields of the products originating from this cleavage parallel the exciplex kinetics behavior of the investigated compounds. And indeed, in the styrene amine systems 2 and 3 in cyclohexane the exciplex decay times are short, and the yields for bond cleavage are relatively high. Upon increasing the solvent polarity, the decay times increase and yields of products decrease. But looking at the results of 8, the opposite behavior can be seen. In acetonitrile, the yield for products is smaller, but the exciplex decay time is shorter than in THF.

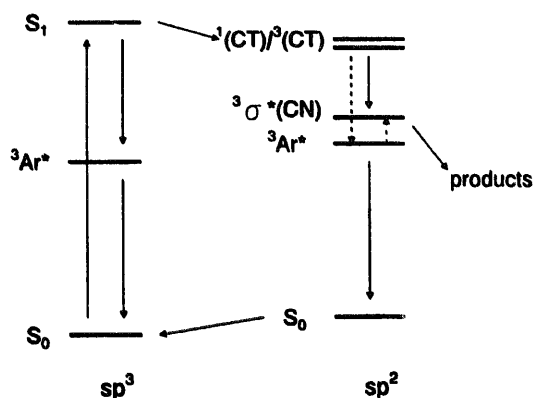
Since the experimental results do not provide a unique answer to the question of the reaction mechanism, theoretical considerations might be useful. One can speculate that for the

Table 5
Quantum yields for product formation from (aminomethyl)arenes in different solvents

Compound	Solvent	$\Phi_{\text{r}}(\text{ArCH}_3)^a$	$\Phi_{\text{r}}(\text{dimer})^a$
2	hexane	0.08	b
	hexane	0.06	b
3	acetonitrile	0.001	b
	hexane	0.06	0.01
4	acetonitrile	0.007	0.005
	hexane	0.075	0.07
5	acetonitrile	0.16	0.064
	hexane	0.030	0.036
6	benzene	0.008	0.005
	acetonitrile	0.0008	0.0008
	hexane	< 0.001	b
7	THF	0.001	b
	acetonitrile	0.007	b
	hexane	0.034	b
8	THF	0.009	b
	acetonitrile	0.003	b

^a The value of Φ_{r} is concentration dependent, estimated error 10%.

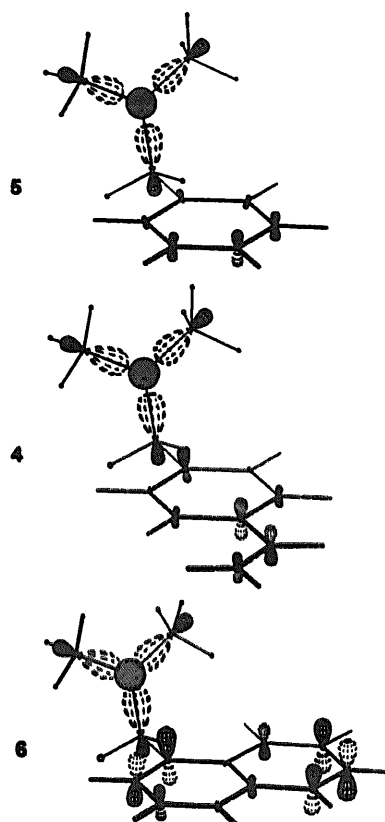
^b Not measured.



Scheme 4. Energy level scheme and proposed excited state deactivation pathways of the (aminomethyl)arene compounds except the benzene derivative (For this compound, the $^3\text{Ar}^*$ state is calculated with larger excitation energy than the $^3\sigma^*(\text{CN})$ state).

different arenes, the energetics of the various states may be important in switching the dominant decay pathways.

In Table 4, the results of the quantum-chemical calculations are listed. For one example, namely compound 4, they are visualized in Scheme 4. The quantity $\Delta(\Delta H_f)$, which is nearly the same in all compounds, refers to the calculated difference in heat of formation if the compound adopts either the optimized geometry or the hypothetical, compact CT geometry as described above. Adding to these values the calculated excitation energies (vertical transition energies) yields the energetic level ordering for both types of geometries. Since planarization of the amino group has no effect on the excitation energy to the localized arene excited states, these will always be lower in energy if the molecule adopts the ground state optimized geometry. The surprising result of the calculations is, however, that the energy of the $^3\sigma^*(\text{CN})$ state varies significantly with the size of the arene moiety. If it were truly localized in the side chain, its energy should be more or less the same for all compounds. As is shown, in Scheme 5, delocalisation of this state into the arene system is small only in the benzene and styrene derivatives, but significant in the larger ones. As a consequence, the energies of the $^3\sigma^*(\text{CN})$ state are similar within the first group of compounds and vary considerably in the second one. Connected with this variation is the variation in energy difference between ^1CT and $^3\text{Ar}^*$ -states, which is in all cases positive and fairly large except in the benzene derivative 5. In view of the possible error in the calculations, this is to say that the locally excited triplet arene state can most likely not act as precursor to the dissociative $^3\sigma^*(\text{CN})$ state, except perhaps in the case of 5 (because the $^3\sigma^*(\text{CN})$ state has some charge transfer character (dipole moment 1–2 D), it will in addition be stabilized better in polar solvents than the triplet arene state). Remarkable in this context is the large difference between the two types of triplet states in derivative 7 (0.92 eV), which is due to the low energy of the arene triplet state and which could be one reason for the exceptional behaviour of this compound (in order to allow a judgement on the



Scheme 5. Corresponding MO orbital of the $^3\sigma^*(\text{CN})$ state of 4, 5 and 6.

quality of the calculated excitation energies, we have included experimentally determined triplet energies in Table 4).

On the other hand, one can also deduce from Table 4 that the energetic difference between ^1CT and $^3\sigma^*(\text{CN})$ state is also subject to large variations, which are not correlated to the size of the arene moiety. The calculated dipole moment in the ^1CT state increases when going from 5 to 8 and, therefore, the stabilisation of this state in polar solvents. Both effects combined can yield a complex dependence of the rates for radiationless transition (energy gap law) when solvent and arene size are changed.

The benzene derivative is a special case with respect to the excitation energies of the triplet states involved, a fact, which could result in a high yield of primary radicals. The exceptionally high yield of toluene can be rationalized also by taking into consideration that the benzyl radical can react with the solvent (hydrogen abstraction) very efficiently without leaving the solvent cage. Therefore, product formation should be higher than in case of the other arenes (a similar yield for bond dissociation assumed) and less dependent on the yield of cage escape.

4. Summary

It is shown that ((*N,N*-dimethylamino)methyl)arenes undergo photoinduced homolytic cleavage of the methylene–nitrogen bond leading primarily to the corresponding methyl

derivatives and the 1,2-diarylethanes. It is proposed that the dissociative $^3\sigma^*$ (CN) state is populated via the charge transfer state (exciplex $AR^- - ^+NR_2$). This hypothesis is, however, difficult to prove experimentally since exciplex emission is generally very weak or even absent in most cases. From the results of quantum chemical model calculations, it is concluded that variations in arene size and solvent polarity change the energy gap between the relevant states in a non uniform way and concomitantly the relative importance of the various decay channels.

Acknowledgements

Financial support by Deutsche Forschungsgemeinschaft, Fonds der Chemie and National Science Foundation is gratefully acknowledged.

References

- [1] E.A. Chendross and H.T. Thomas, *Chem. Phys. Lett.*, **5** (1971) 393.
- [2] D. Bryce-Smith, A. Gilbert and G. Klunklin, *J. Chem. Soc., Chem. Comm.*, (1973) 330.
- [3] (a) D.R.G. Brimage and R.S. Davidson, *Chem. Comm.*, (1971) 1385; (b) R.S. Davidson and K.R. Trethewey, *J. Chem. Soc., Chem. Comm.*, (1976) 827. (c) R.A. Beecroft, R.S. Davidson, D. Goodwin and J.E. Pratt, *Pure Appl. Chem.*, **54** (1982) 1605.
- [4] (a) M. Van der Auweraer, A. Gilbert and F.C. De Schryver, *J. Am. Chem. Soc.*, **102** (1980) 4007; 4(b) Ph. Van Haver, N. Helsen, S. Depaemelaere, M. Van der Auweraer and F.C. de Schryver, *J. Am. Chem. Soc.*, **193** (1991) 6849; (c) B. Wegewijs, R.M. Hermont, J.W. Verhoeven, M.A. De Haas and J.M. Warman, *Chem. Phys. Lett.*, **168** (1990) 185.
- [5] (a) F.D. Lewis, G.D. Reddy, S. Schneider and M. Gahr, *J. Am. Chem. Soc.*, **113** (1991) 3498; (b) F.D. Lewis, G.D. Reddy, D.M. Bassani, S. Schneider and M. Gahr, *J. Photochem. Photobiol. A: Chem.*, **65** (1992) 205; (c) F.D. Lewis, G.D. Reddy, D.M. Bassani, S. Schneider and M. Gahr, *J. Am. Chem. Soc.*, **116** (1994) 597.
- [6] F.D. Lewis and B.E. Cohen, *J. Phys. Chem.*, **89** (1994) 10 591.
- [7] S. Schneider, H. Rehaber, M. Gahr and W. Schüßlbauer, *J. Photochem. Photobiol. A: Chem.*, **82** (1994) 129.
- [8] M.A. Ratcliff Jr. and J.K. Kochi, *J. Org. Chem.*, **37** (1972) 3268.
- [9] (a) H. Rehaber, *Masters Thesis*, Universität Erlangen (1993); (b) J.P. Monthéard, B. Boinon and B. Benayad, *Makromol. Chem. Rapid. Commun.*, **8** (1982) 255.
- [10] R.F. Borch and A.I. Hassid, *J. Org. Chem.*, **37** (1972) 1673.
- [11] F.D. Lewis and D.J. Johnson, *J. Photochem.*, **7** (1977) 421.
- [12] J.I. Seeman, V.H. Grassian and E.R. Bernstein, *J. Am. Chem. Soc.*, **110** (1988) 8542.
- [13] (a) G. Rauhut, A. Alex, J. Chandrasekhar and T. Clark, *Vamp 5.5*, Erlangen 1994; (b) J.J.P. Stewart, *J. Comput. Chem.*, **10** (1989) 209.
- [14] (a) D. Rehm and A. Weller, *Isr. J. Chem.*, **8** (1970) 259; (b) A. Weller, *Z. Phys. Chem.*, **133** (1982) 92.
- [15] E. Lippert, *Z. Elektrochem.*, **61** (1957) 962.
- [16] M. Gahr, *PhD Thesis*, Universität Erlangen (1993).
- [17] T. Okada, I. Karaki, E. Matsuzawa, N. Mataga, Y. Sakata and S. Misumi, *J. Phys. Chem.*, **85** (1981) 3956.
- [18] T.-C. Mai, Y.-C. Lin, T.-M. Hseu and T.-I. Ho, *J. Photochem. Photobiol. A: Chem.*, **71** (1993) 237.
- [19] S.L. Murov, I. Carmichael and G.L. Hug, *Handbook of Photochemistry*, 2nd ed., M. Dekker, New York, 1993, p. 269 ff.
- [20] J.A. Riddick, W.B. Bunger and Th.K. Sakano, in *Technics of Chemistry. Organic Solvents*, Vol. II, 4th ed., Wiley and Son, New York, 1986, pp. 583 and 657.